JOURNAL OF VIROLOGY, Apr. 2002, p. 3125–3134 Vol. 76, No. 7
0022-538X/02/$04.00+0 DOI: 10.1128/JVI.76.7.3125–3134.2002

Capsid-Specific Cytotoxic T Lymphocytes Recognize Three Distinct H-2D^b-Restricted Regions of the BeAn Strain of Theiler's Virus and Exhibit Different Cytokine Profiles

Michael A. Lyman, Hee-Gu Lee,† Bong Su Kang, Hee-Kap Kang, and Byung S. Kim*

Department of Microbiology-Immunology and Institute of Neuroscience, Northwestern University Medical School, Chicago, Illinois 60611

Received 21 August 2001/Accepted 2 January 2002

The role of virus-specific cytotoxic T lymphocytes (CTL) in Theiler's murine encephalomyelitis virus (TMEV)-induced demyelinating disease, a viral model for multiple sclerosis, is not yet clear. To investigate the specificity and function of CTL generated in response to TMEV infection, we generated a panel of overlapping 20-mer peptides encompassing the entire capsid and leader protein region of the BeAn strain of TMEV. Binding of these peptides to H-2K^b and H-2D^b class I molecules of resistant mice was assessed using RMA-S cells. Several peptides displayed significant binding to H-2K^b, H-2D^b, or both. However, infiltrating cytotoxic T cells in the central nervous system of virus-infected mice preferentially lysed target cells pulsed with VP2$_{111–130/121–140}$ or VP2$_{121–130}$, a previously defined CTL epitope shared by the DA strain of TMEV and other closely related cardioviruses. In addition, at a high effector-to-target cell ratio, two additional peptides (VP2$_{161–180}$ and VP3$_{101–120}$) sensitized target cells for cytolysis by infiltrating T cells or splenic T cells from virus-infected mice. The minimal epitopes within these peptides were defined as VP2$_{165–173}$ and VP3$_{110–120}$. Based on cytokine profiles, CTL specific for these subdominant epitopes are Tc2, in contrast to CTL for the immunodominant epitope, which are of the Tc1 type. Interestingly, CTL function towards both of these subdominant epitopes is restricted by the H-2D molecule, despite the fact that these epitopes bind both H-2K and H-2D molecules. This skewing toward an H-2D^b-restricted response may confer resistance to TMEV-induced demyelinating disease, which is known to be associated with the *H-2D* genetic locus.

Although the etiology of multiple sclerosis (MS) remains unknown, epidemiological studies and animal models have supported a potential role for viruses as causative agents of demyelination (1, 7, 10). One such virus is Theiler's murine encephalomyelitis virus (TMEV), a common enteric mouse picornavirus. Members of the Theiler's original (TO) subgroup of TMEV, such as the BeAn and DA strains, induce a biphasic disease when injected into the central nervous system (CNS) of susceptible strains of mice. While the early mild encephalitogenic phase is clinically undetectable for the BeAn strain, both of these TO strains eventually induce a chronic, progressive demyelinating disease that is similar clinically and histopathologically to human MS (27). In addition, TMEV infection of demyelination-susceptible mice leads to eventual immune responses against myelin autoantigens (31). Furthermore, the various immunological and genetic factors that affect disease outcome in mice closely parallel those associated with the development of MS in humans (21). Combined with a suspected viral etiology for MS (1, 10, 46), these similarities make TMEV a relevant infectious model for the study of this human autoimmune disease.

Demyelination induced in the highly susceptible SJL/J mouse strain following intracerebral infection with TMEV is associated with virus persistence in the CNS (4, 28, 45), and CD4$^+$ Th1-type responses to viral epitopes (16, 53) apparently play a critical role in the immunopathologic tissue damage. The CD4$^+$ T-cell epitopes in this mouse strain have been identified on the VP1, VP2, and VP3 capsid proteins (15, 51, 52), which form the external structure of the virus. While similar mapping studies have been done for the antibody response to TMEV (18, 20), the role of antibodies in demyelination remains unclear. Even less well characterized is the role of virus-specific CD8$^+$ cytotoxic T lymphocytes (CTL).

Resistance to demyelination is closely linked to the major histocompatibility complex (MHC) class I genetic locus (5, 44), suggesting that class I-restricted CD8$^+$ T cells may be important mediators of protection in resistant strains or of pathogenesis in susceptible mice. One group of investigators has suggested that CD8$^+$ T cells are required for the development of disease, based on the observation that β_2-microglobulin-deficient and perforin-deficient mice, despite exhibiting significant demyelination, fail to show clinical signs of disease (32, 43). In contrast, our previous studies (36, 40) with the same deficient strains suggest that perforin-mediated lysis by CD8$^+$ CTL is not required for disease. In our hands, these mice mount increased CD4$^+$ T-cell proliferative and delayed-type hypersensitivity responses to viral antigens, and while most of these mice show subclinical demyelination, subcutaneous immunization with UV-inactivated TMEV leads to full-blown demyelinating disease even in the absence of CD8$^+$ T cells or perforin-mediated lytic function. Thus, this remains a controversial issue.

Moreover, *H-2D$^{b-/-}$* mice on the resistant C57BL/6 back-

* Corresponding author. Mailing address: Department of Microbiology-Immunology, Northwestern University Medical School, 303 E. Chicago Ave., Chicago, IL 60611. Phone: (312) 503-8693. Fax: (312) 503-1339. E-mail: bskim@northwestern.edu.

† Permanent address: Virus Oncology Research Unit, Molecular and Cell Biology, Research Division, Korea Research Institute of Bioscience and Biotechnology, Taejon 305-600, South Korea.

ground are susceptible to persistent virus infection (2), while *H-2K*$^{b-/-}$ mice are not. Taken together, these data suggest that an H-2D^b-restricted CTL response is likely involved in virus clearance and is not required for the development of demyelination. Finally, adoptive transfer of CD8$^+$ T cells was able to confer resistance to TMEV-induced demyelinating disease in susceptible recipient mice (33), again supporting the protective role of this cell population. However, the specificity of the CD8$^+$ T cells in these studies remains unknown. Thus, in order to understand the exact role of TMEV-specific CD8$^+$ T cells in either resistant or susceptible strains, the specificity and effector function of these virus-specific CD8$^+$ T cells must first be characterized.

The potential role of CTL was initially investigated using virus-infected cells as target cells, and the cytotoxic function of CNS-infiltrating lymphocytes was demonstrated in resistant as well as susceptible mice (26, 37, 39). Using the DA strain of Theiler's virus, Rodriguez and colleagues reported that cells from the spinal cords of resistant C57BL/10 mice specifically lyse target cells expressing VP1 and VP2, but not VP3 (25). Subsequently, the VP2$_{121–130}$ region of the DA strain was independently identified by two separate groups as a predominant CTL epitope (3, 9) and appears to constitute greater than 50% of CNS-infiltrating CD8$^+$ T cells (19). However, the other inferred CTL epitopes have not yet been identified. In addition, no such CTL epitopes have been reported for the BeAn strain of Theiler's virus, which is similar to but distinct from the DA strain in both genome sequence (85% identity at the nucleotide level) and pathogenicity.

As CTL recognize peptides from immunogenic proteins in association with MHC class I molecules, an obvious prerequisite for a potential T-cell epitope is MHC class I binding. In this study, we have used this requirement of MHC class I binding to search for potential CTL epitopes within the P1 region of the TMEV polyprotein, which includes the leader and the VP1, VP2, VP3, and VP4 capsid proteins. Using a library of overlapping 20-mer peptides encompassing the entire P1 region, we have identified the peptides that can bind the H-2D^b and H-2K^b molecules. The use of 20-mer peptides here has led to the identification of two new subdominant H-2D^b-restricted CTL epitopes in C57BL/6 mice. Further functional analysis of the T cells specific for these epitopes, which lie on VP2 and VP3, will be discussed.

MATERIALS AND METHODS

Animals. Female C57BL/6 mice were purchased from the National Cancer Institute, Frederick, Md. All mice were housed at the Animal Care Facility of Northwestern University.

Viruses and cell lines. The BeAn strain of TMEV was propagated in, and its titer was determined on, BHK cells grown in Dulbecco's modified Eagle's medium supplemented with 7.5% donor calf serum. The RMA-S (*H-2^b*), EL4 (*H-2^b*), L929-D^b, and L929-K^b cell lines were maintained in RPMI 1640 supplemented with 10% fetal calf serum, glutamine-pyruvate, and antibiotics. RMA-S cells were obtained from Jeffrey Bluestone with permission from Klas Karre (48). The L929-D^b and L929-K^b cell lines were a kind gift from David Woodland.

Synthetic peptides and MHC stabilization assays. Synthetic peptides were generated with the RaMPS peptide synthesis system (Du Pont Co., Wilmington, Del.). All peptides were dissolved in dimethyl sulfoxide before dilution. For MHC-binding assays, RMA-S cells were loaded with various peptides (40 μM) for 16 to 18 h at 37°C. Levels of surface class I molecules were assessed by flow cytometric analysis (FACScan; Becton Dickinson) using mouse monoclonal antibodies specific for H-2K^b (Y-3) and H-2D^b (28-14-8S). followed by fluorescein isothiocyanate-labeled anti-mouse immunoglobulin antibodies (Biosource, Camarillo, Calif.).

Infection of mice with TMEV. For intracerebral infection, 30 μl (approximately 10^5 PFU) of TMEV BeAn was injected into the right cerebral hemisphere of 6- to 8-week-old mice anesthetized with methoxyflurane.

Isolation of CNS-IL. Mice were anesthetized with methoxyflurane and perfused through the left ventricle with 30 ml of sterile Hanks' balanced salt solution (HBSS). Brains and spinal cords were removed and placed in cold HBSS. Tissues were forced through wire mesh and incubated at 37°C for 45 min in 250 μg of collagenase type 4 (Worthington Biochemical Corp., Lakewood, N.J.) per ml. Cell suspensions were then washed, resuspended in 20 ml of HBSS, and mixed with 10 ml of Percoll. CNS-infiltrating lymphocytes (CNS-IL) were isolated from a continuous Percoll (Pharmacia, Piscataway, N.J.) gradient after centrifugation for 30 min at 27,000 × *g*.

For CTL assays, cells were washed with RPMI 1640 and plated in wells of a 24-well plate overnight in RPMI 1640 with 5% fetal calf serum, glutamine-pyruvate, nonessential amino acids, and β-mercaptoethanol (RPMI-5) and 5 U of recombinant interleukin-2 (IL-2). Cells were used as effectors the next day in a standard ^{51}Cr release assay. For Elispot analysis, cells were washed, resuspended in HL-1 medium (Bio-Whittaker, Walkersville, Md.), and used on the same day.

CTL assays. All target cells were incubated overnight with 20-mer peptides or for 4 to 6 h with truncated peptides. Nonadherent RMA-S and EL4 cells were labeled with ^{51}Cr (50 μCi per target) for the last 2 h of incubation on the day of the assay. After three washes with RPMI 1640, target cells were resuspended at 3×10^4 cells/ml in RPMI-5. Cells were added to a 96-well round-bottomed plate at 100 μl/well. Adherent L929-D^b and L929-K^b target cells were ^{51}Cr labeled for 2 h on the day before CTL assays were performed. Cells were trypsinized, labeled, washed, and plated at 2.5×10^3 cells/well in 96-well round-bottomed plates. Cells were incubated overnight to allow adherence to the plate. On the day of assay, wells were washed once by aspirating off old medium and replacing it with fresh RPMI-5.

CNS effector cells and in vitro-stimulated spleen cells were harvested from 24-well plates, and dead cells were removed with Histopaque (Sigma, St. Louis, Mo.) centrifugation. Cells were washed and resuspended in RPMI-5, and 100 μl was added to target cells at different dilutions. Plates were spun at 353 × *g* for 1 min to initiate cell-cell contact. Supernatants were harvested after 6 h of incubation at 37°C, and mean radioactivity values were calculated for duplicate wells. Percent specific lysis was calculated according to the standard formula [(experimental counts − spontaneous counts)/(maximum counts − spontaneous counts)] × 100. Spontaneous release for all experiments was <15%.

Cytokine Elispot assays. Elispot plates (Millipore, Bedford, Mass.) were coated with 1 to 5 μg of anti-gamma interferon (IFN-γ) antibody or anti-IL-5 antibody per ml in 0.05 M carbonate-bicarbonate buffer (pH 9.6). Plates were washed and then blocked with sterile phosphate-buffered saline (PBS) containing 1% bovine serum albumin (BSA). Plates were incubated with 1×10^4 to 2×10^4 CNS-IL plus 1×10^6 naive syngeneic spleen cells (3,000 rads) in 200 μl at 37°C under 5% CO_2 for 18 h (IFN-γ) or 40 h (IL-5) with 2 μM peptide. Optimal incubation times were predetermined for each cytokine. IFN-γ and IL-5 spots were developed as previously described using biotin-conjugated anticytokine antibodies (Endogen, Boston, Mass.) and streptavidin-horseradish peroxidase in 1% BSA–PBS (47).

RESULTS

Identification of the 20-mer peptides capable of binding H-2K^b and/or H-2D^b class I molecules. To identify potential CTL epitopes within the structural proteins of the BeAn strain of TMEV, 20-mer peptides overlapping by 10 amino acids each were synthesized based on the previously reported sequence of the P1 region that encodes the leader and capsid proteins (22, 38). These 20-mer peptides (20 μM) were incubated with the TAP1-deficient RMA-S cell line. Incubation of RMA-S cells with H-2D^b- or H-2K^b-binding peptides has been shown to enhance surface expression of the respective MHC class I molecules on these cells by stabilizing the peptide-MHC complex (29). Thus, peptide-pulsed cells were analyzed for cell surface expression of MHC class I using monoclonal antibodies specific for H-2D^b or H-2K^b molecules.

While incubation with most peptides resulted in low or no

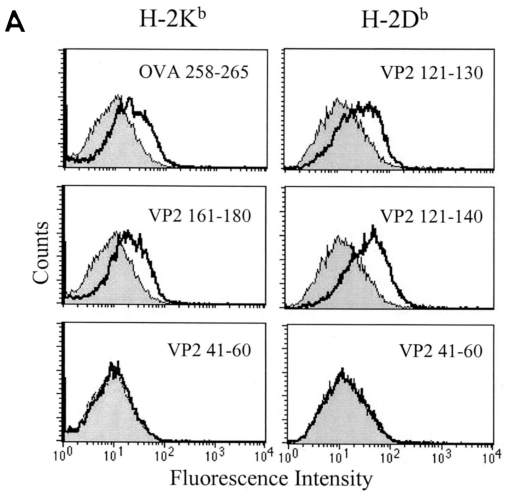

FIG. 1. Assessment of binding of 20-mer peptides within the BeAn P1 region to H-2K^b and H-2D^b molecules. (A) Examples of peptide binding assessment, including the known K^b-binding ($OVA_{258–265}$) and D^b-binding ($VP2_{121–130}$) peptides as positive controls. $VP2_{161–180}$ and $VP2_{121–140}$ represent K^b- and D^b- binding peptides, respectively. $VP2_{41–60}$ is an example of a nonbinding peptide. Shaded histograms represent MHC class I expression in the absence of peptide, and open histograms represent class I expression after incubation with the indicated peptide. (B) K^b- and D^b-binding profile of the overlapping peptides covering the entire P1 (leader, VP4, VP2, VP3, and VP1) region. Mean fluorescence intensity (MFI) difference = MFI with peptide − MFI without peptide.

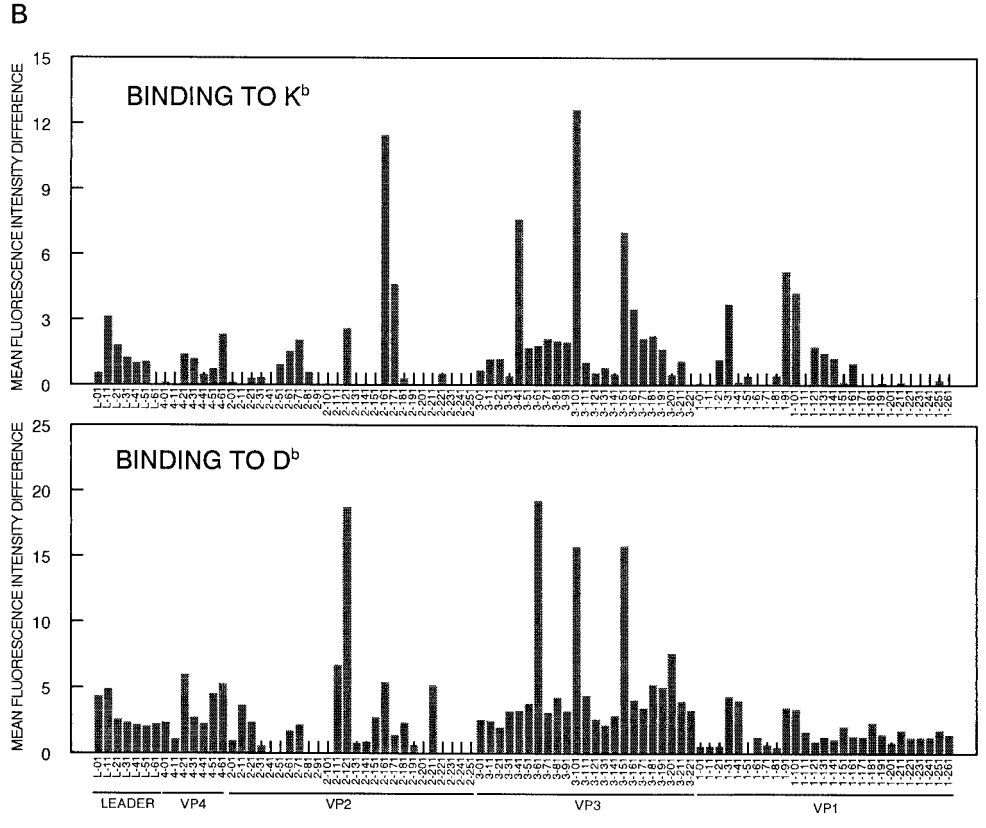

expression of MHC class I molecules above that seen in the absence of peptide, some peptides displayed clear H-2K or H-2D binding as detected by increased MHC class I surface expression (Fig. 1, Table 1). While the mechanisms involved in the stable binding of the 20-mer peptides to the class I molecules are not clear, others have shown that peptides longer than 8 to 11 amino acids (the traditional MHC class I binding peptide length) can stabilize RMA-S class I expression (11, 42). Use of 20-mer peptides here provided a level of detection of class I binding similar to that attained using a minimal 10-mer epitope, since $VP2_{111–130}$ (not shown) and $VP2_{121–140}$ (Fig. 1A) induced levels of D^b expression similar to those induced by the previously defined $VP2_{121–130}$ epitope (3). Analysis of class I binding indicates the presence of three categories of class I binding peptides within the P1 library (Fig. 1B). Peptides in the first category ($VP2_{161–180/171–190}$, $VP3_{41–60}$, and $VP1_{91–110/101–120}$) preferentially bind to H-2K^b, while those in the second category ($VP2_{111–130/121–140}$ and $VP3_{61–80}$) interact only with H-2D^b molecules. The third category ($VP3_{101–120}$ and $VP3_{151–170}$) binds both H-2K^b and H-2D^b, as suggested by enhancement of surface expression of both of these class I molecules.

TABLE 1. Summary of peptide sequence, binding activity, and CTL function for the MHC class I-binding P1 region peptides

Peptide	Binding[a]	CTL response[b]	Sequence
$VP1_{91–110}$	K^b	−	VQWRWVRSGG VNGANFPLMT
$VP1_{101–120}$	K^b	−	VNGANFPLMT KQDYAFLCFS
$VP2_{111–130}$	D^b	+++	RVQVQCNASQ FHAGSLLVFM
$VP2_{121–140}$	D^b	+++	FHAGSLLVFM APEFYTGKGT
$VP2_{161–180}$	$K^b > D^b$	+	QGAPTGYRU SRTGFFATNH
$VP3_{41–60}$	K^b	−	FSDLLELCKL PTFLGNPTNP
$VP3_{61–80}$	D^b	−	NKRYPYFSAT NSVPATSMVD
$VP3_{101–120}$	K^b and D^b	+	NFNQYRGSLN FLFVFTGAAM
$VP3_{151–170}$	K^b and D^b	−	WDLGLNSSFN FTAPFISPIH

[a] Peptides that induced a substantial increase in MHC expression (MFI difference >7) are shown here.

[b] +, mean value of >5% and <20%; +++,> 30% specific lysis above background for five experiments.

TMEV infection induces CTL recognizing one dominant ($VP2_{121–130}$) and two subdominant ($VP2_{161–180}$ and $VP3_{101–120}$) epitopes. To identify new CTL epitopes among the H-2K^b- and H-2D^b-binding peptides, RMA-S cells loaded with these peptides were used to assess the CTL activity of CNS-IL 8 days after intracerebral infection with BeAn virus. Due to the low numbers of mononuclear cells obtainable from the CNS of a TMEV-infected mouse ($\sim 1 \times 10^5$ to 2×10^5), low effector-to-target cell (E:T) ratios (20:1 and 2:1) were used initially. Of all the class I binding 20-mer peptides, only $VP2_{111–130}$ and $VP2_{121–140}$ were able to sensitize RMA-S targets for lysis by CNS-IL at these low E:T ratios (Fig. 2A). Since these two peptides both contain the previously identified $VP2_{121–130}$ CTL epitope of the DA virus (3, 9), this 10-mer peptide was used to confirm that CTL from BeAn-infected mice recognize the same epitope as those from DA-infected mice. Our results (Fig. 2A) clearly indicate that infiltrating CTL in the CNS of mice infected with BeAn virus recognize the identical epitope region ($VP2_{121–130}$) as CTL from DA virus-infected mice.

To examine the possibility that other subdominant epitopes may exist, we repeated our assays for CTL function at higher E:T ratios. Using a similar panel of peptides as in Fig. 2A, we found that two additional peptides, $VP2_{161–180}$ and $VP3_{101–120}$, were able to sensitize RMA-S target cells (or EL4 cells; data not shown) for lysis by CNS-IL from TMEV-infected mice at an E:T of 80:1 (Fig. 2B). In addition, splenic T cells from virus-infected mice that were further stimulated in vitro with either $VP2_{161–180}$ or $VP3_{101–120}$ displayed enhanced cytolytic activity against the respective peptides, while splenic T cells stimulated with other class I binding peptides (e.g., $VP1_{91–110}$ and $VP3_{151–170}$) showed no significant CTL activity against these peptides (Fig. 3).

Since RMA-S cells do not express surface class II molecules (50), the observed cytotoxicity most likely represents class I-restricted, TMEV-specific CTL function. In fact, further assessment of CNS-infiltrating cell populations selected positively or negatively with magnetic cell separation confirmed that the CD8$^+$ T-cell population delivers the virus-specific cytotoxicity (data not shown). These results suggest that CD8$^+$ CTL specific for the subdominant epitopes are present in CNS as well as the peripheral lymphoid organs of virus-infected mice. It should be noted that CTL activity against these two epitopes was not observed in every experiment. While $VP3_{101–120}$-specific CTL have been detected in more than 70% of our experiments (11 of 15), the $VP2_{161–180}$-specific response was seen less frequently (5 of 15). Thus, an immunodominance hierarchy exists as follows: $VP2_{121–130} > VP3_{101–120} > VP2_{161–180}$.

$VP2_{165–173}$ and $VP3_{110–120}$ represent H-2D^b-restricted minimal CTL epitopes. To determine the minimal epitopes recognized by CTL specific for $VP2_{161–180}$ and $VP3_{101–120}$, we generated truncated forms of these peptides and assessed which truncated peptides could sensitize target cells for lysis by either CNS-IL or in vitro-stimulated splenic T cells from TMEV-infected C57BL/6 mice. Within $VP2_{161–180}$, one 9-mer peptide corresponding to $VP2_{165–173}$ (TGYRYDSRT) most closely matched the known K^b binding motif (41). Since $VP2_{161–180}$ appeared to bind K^b better than D^b (Fig. 1), and since no sequence within this region matched the known D^b binding motif, we predicted that this peptide might represent a K^b-restricted minimal CTL epitope within $VP2_{161–180}$. As shown in Fig. 4A, $VP2_{165–173}$ sensitized RMA-S cells for lysis by CNS-IL from virus-infected mice, as predicted. In order to determine the MHC restriction of these CTL, we used target cell lines expressing only H-2K^b or H-2D^b (6, 35). To our surprise, $VP2_{165–173}$-specific killing appears to be restricted by D^b rather than K^b, since L929-D^b transfectants but not L929-K^b transfectants were killed in a peptide-specific manner (Fig. 5A).

Since no clear class I binding motif exists within $VP3_{101–120}$ and this peptide binds both H-2D^b and H-2K^b molecules (Table 1), a panel of truncated peptides was generated in order to determine the minimal epitope within this region. Of all the truncated peptides, only $VP3_{110–120}$ (NFLFVFTGAAM) sensitized target cells for lysis (Fig. 4B). Since this peptide consists of 11 amino acids, shorter peptides were generated to precisely define the minimal epitope. However, unlike the 11-mer, these shorter peptides ($VP3_{111–120}$ and $VP3_{112–120}$) were unable to sensitize target cells for lysis by CNS-IL (data not shown), suggesting that $VP3_{110–120}$ represents the minimal CTL epitope. Interestingly, even though $VP3_{104–120}$ contains this 11-mer sequence, effector CTL did not lyse target cells pulsed with this longer peptide. Also, the 20-mer $VP3_{101–120}$ appears to be more efficient than $VP3_{110–120}$ at sensitizing target cells for lysis. Although the reason(s) for this is unclear, it likely involves the different solubilities of these different-sized hydrophobic peptides.

As before, we used L929-D^b and -K^b transfectants to determine the MHC class I restriction element for this VP3 epitope. Because the 20-mer $VP3_{101–120}$ more efficiently sensitized target cells for CTL-mediated lysis in the previous experiments, we used this peptide instead of $VP3_{110–120}$ in subsequent experiments. As shown in Fig. 5B, the D^b class I molecule clearly restricts this CTL response. Thus, despite efficient binding to the K^b class I molecule, both of the epitopes defined here represent subdominant, H-2D^b-restricted CTL epitopes.

Dominant and subdominant epitopes induce differential cytokine production. In addition to lysing infected target cells, CD8$^+$ T cells may also secrete various cytokines in response to foreign pathogens. To analyze cytokine responses to the three CTL epitopes, IFN-γ (a Tc1 type cytokine) and IL-5 (Tc2) production by magnetic bead-isolated CD8$^+$ CNS-IL from virus-infected mice was assessed by an Elispot assay at 8 days

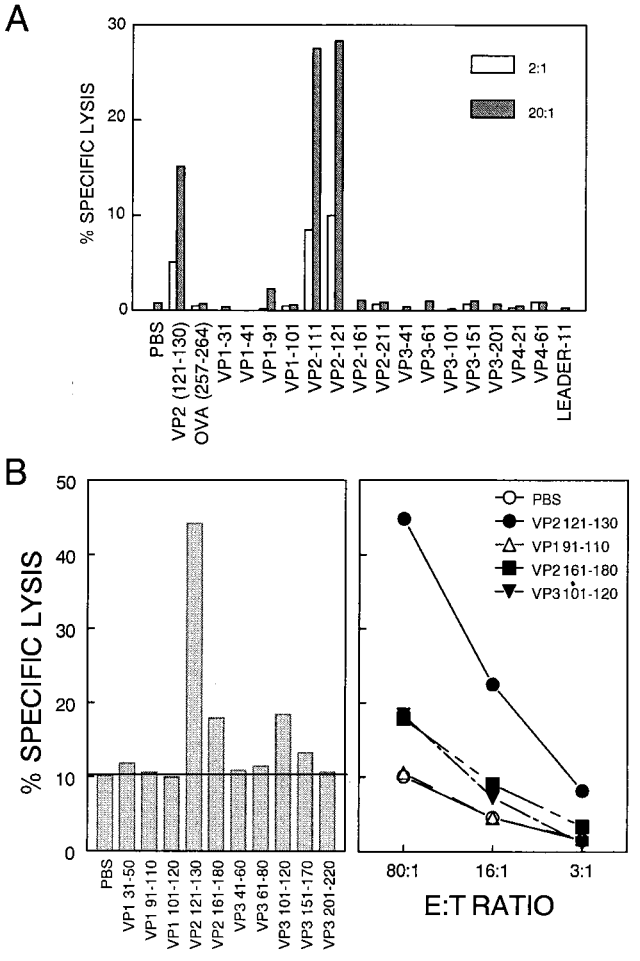

FIG. 2. Ex vivo assessment of lytic function of infiltrating T cells in the CNS from BeAn-infected C57BL/6 mice against target cells loaded with the class I binding peptides. (A) The peptides capable of binding to H-2^b class I molecules were loaded in RMA-S target cells, and specific cytolysis by CNS-infiltrating T cells from virus-infected mice (8 days postinfection) was determined at different E:T ratios. $VP2_{121–130}$, which is identical to the previously reported DA virus epitope, was able to sensitize RMA-S cells for lysis and likely represents the minimal epitope within $VP2_{111–130/121–140}$. (B) To identify potential subdominant CTL epitopes, cytotoxicity at a higher E:T ratio (80:1) was examined (left panel). The right panel shows cytolytic activity at both high and low E:T ratios. Low but significant levels (>5% or 2 SD above background) of cytolysis were observed with target cells loaded with two additional peptides ($VP2_{161–180}$ and $VP3_{101–120}$). Spontaneous release was less than 10%. Data are representative of multiple (>5) experiments.

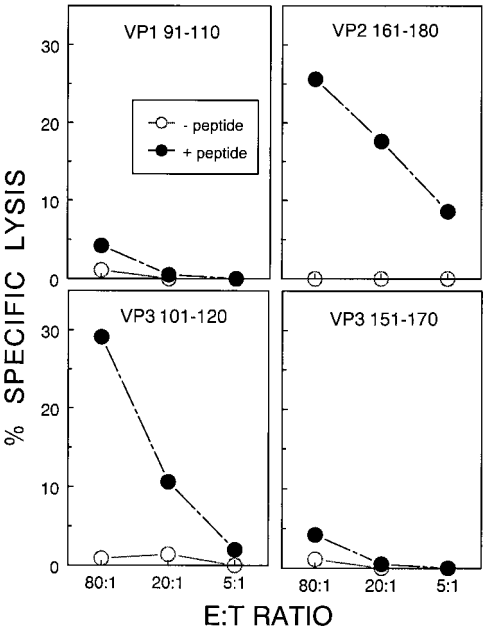

FIG. 3. In vitro expansion of subdominant epitope-specific CTL from splenic T cells of virus-infected mice. Spleen cells from BeAn-infected mice at 8 days postinfection were stimulated for 5 days with the indicated peptide and used as effector cells in a 6-h ^{51}Cr release assay. RMA-S cells loaded with stimulating peptide or unloaded cells were used as target cells. No lysis was observed against control peptides. Spontaneous release was less than 13%.

postinfection. While T cells specific for $VP2_{121–130}$ preferentially produced IFN-γ, $VP2_{161–180}$ and $VP3_{101–120}$ induced production of predominantly IL-5 (Fig. 6). Also, the overall number of spots correlated well with the level of specific lysis against the respective epitopes when effector cells from the same group of mice were analyzed for cytokine production and lytic activity (data not shown). In addition, the overall number of cytokine-producing T cells specific for each epitope in four separate experiments is consistent with the immunodominance hierarchy: $VP2_{121–130}$ (110 ± 40 T cells) > $VP3_{101–120}$ (32 ± 14) > $VP2_{161–180}$ (12 ± 5). Thus, the predominant $CD8^+$ T-cell response is primarily a Tc1 type of response, while the response to the two newly defined subdominant epitopes is primarily Tc2. Although interesting, the significance of this differential cytokine production remains unclear.

To examine the possibility that CNS-IL populations from TMEV-infected animals might contain nonlytic, cytokine-producing $CD8^+$ T cells specific for other capsid protein epitopes, we performed Elispot analysis with the entire P1 peptide library. Although several peptides induced cytokine production by class II-restricted $CD4^+$ T cells, $CD8^+$ T-cell responses to other peptides were not observed (data not shown). These data suggest that the overall $CD8^+$ T-cell response against the leader and capsid proteins of TMEV is directed toward only three distinct epitope regions.

Dominance hierarchy of CTL response is maintained throughout the course of TMEV infection and during recall response. The peak CTL response to TMEV in C57BL/6 mice is observed between 7 and 10 days postinfection. While the dominant response is directed against $VP2_{121–130}$ during this time, it is possible that the immune response may be directed toward different epitopes at different times during the course of virus infection. To address this possibility, we analyzed the CTL response against all three epitopes at 8, 23, and 40 days postinfection (Fig. 7). While a strong CTL response against the dominant epitope was observed early, this response waned by day 23 and remained low at day 40. A low but detectable response against $VP3_{101–120}$ was observed early, but disappeared by day 23. No CTL response was observed against $VP2_{161–180}$ at any of the time points for this particular experiment.

The overall reduction in virus-specific $CD8^+$ T cells in the CNS at 23 and 40 days after virus infection appears to reflect

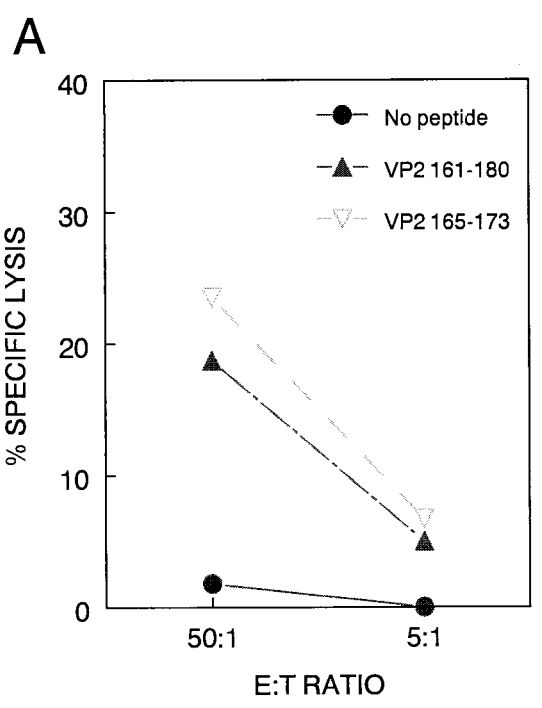

B

Peptide	Lysis
VP3 101-120	++ (23%)
VP3 101-112	-
VP3 103-112	-
VP3 104-111	-
VP3 104-112	-
VP3 104-113	-
VP3 104-120	-
VP3 105-112	-
VP3 105-113	-
VP3 105-114	-
VP3 106-114	-
VP3 106-115	-
VP3 107-116	-
VP3 107-118	-
VP3 109-116	-
VP3 110-120	+ (12%)

FIG. 4. Identification of the minimal CTL epitopes within $VP2_{161–180}$ and $VP3_{101–120}$. (A) The $VP2_{165–173}$ (TGYRYDSRT) peptide was synthesized based on the K^b binding motif and compared with $VP2_{161–180}$ for its ability to sensitize RMA-S target cells for lysis by CTL from the CNS of TMEV-infected mice. Spontaneous release was <9%. (B) A panel of truncated peptides spanning $VP3_{101–120}$ was synthesized and used to identify the minimal epitope within this region. Ex vivo lytic activity of CNS-IL was tested against peptide-loaded or unloaded target cells (E:T = 30:1). Spontaneous release was less than 12%.

reduced numbers of infiltrating $CD8^+$ T cells (unpublished observation). Nevertheless, our results clearly indicate that such $CD8^+$ T-cell responses to subdominant epitopes are not increased over those specific for the dominant epitope during the course of infection. In addition, we analyzed the recall CTL response to TMEV in mice that were infected a second time 33 days after the primary infection (Fig. 7). The secondary response following this repeat infection was nearly identical to that seen very early (8 days). These data suggest that the immunodominance hierarchy is maintained throughout the course of TMEV infection as well as during the recall response to subsequent virus challenge.

DISCUSSION

Various methods have been employed for mapping pathogen-specific class I-restricted CTL epitopes. The most common method involves the expression of potential CTL target proteins in cell lines for use as target cells in CTL assays (8, 49). Synthetic peptides are then used to determine the exact minimal epitope within a given antigenic protein. Although others have used similar methods to map the immunodominant TMEV CTL epitope in C57BL mice (3, 25), we have found it very difficult to generate stable transfectants expressing Theiler's virus capsid proteins. The reason for this apparent instability is not clear.

Another method for determining CTL epitopes makes use of sequence motifs that characterize the peptides that associate with different MHC class I molecules (41). Our search of the TMEV protein sequence (≈2,300 amino acids) revealed several potential $H\text{-}2^b$ class I binding peptides. However, none of these peptides appear to be T-cell epitopes in C57BL/6 mice as detected by our CTL assays (unpublished observation). Thus, the predictive value of MHC binding motifs does not always prove reliable. Furthermore, not all class I-restricted epitopes adhere to the reported binding motif of their restricting MHC molecule. In fact, neither the $VP2_{165–173}$ epitope nor the $VP3_{110–120}$ epitope exactly matches the reported $H\text{-}2D^b$ motif.

Although the presence of multiple CTL epitopes has been suggested for the C57BL/6 strain, only one of these epitopes has been defined for Theiler's virus. In the present study, we assessed the binding of 20-mer peptides to the D^b and K^b molecules as a means to define potential new CTL epitopes (Fig. 1). Although class I binding peptides are usually smaller peptides of 8 to 11 amino acids, the use of 20-mer peptides here reduced the number of peptides required (only 90 peptides) to screen the 922-amino-acid P1 region. Others have also shown that longer peptides can stabilize surface expression of MHC molecules on RMA-S cells (11, 42), although the mechanism for this phenomenon is unknown. Possible mechanisms may include any one or a combination of the following: additional TAP-independent processing of the 20-mers by the RMA-S cells (30), cleavage of the 20-mers into shorter peptides by serum proteases during overnight incubation (13, 23), or the presence of contaminating truncated peptides in the synthetic 20-mer preparations.

We report here that two 20-mer peptides containing the

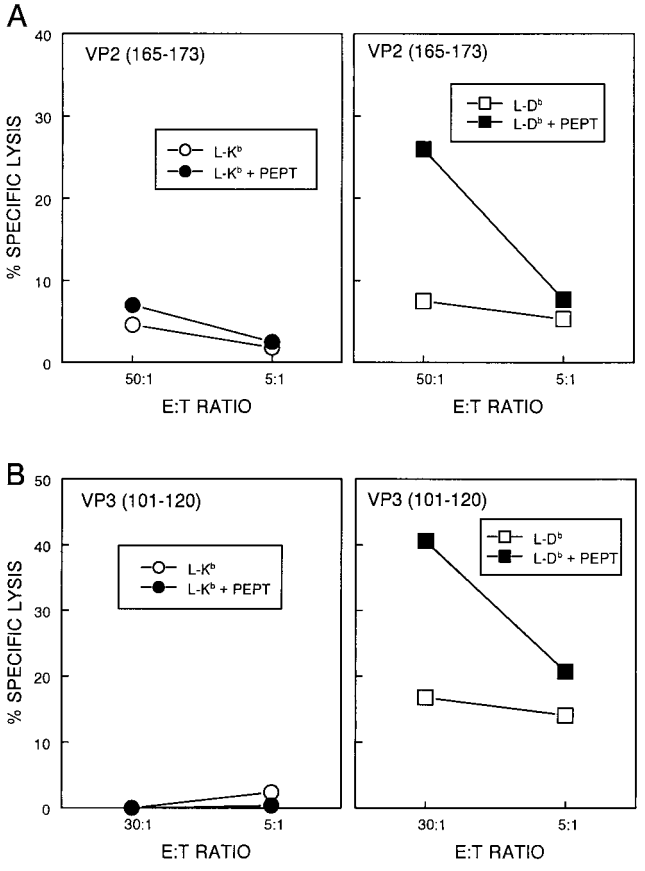

FIG. 5. Determination of MHC class I restriction element for subdominant CTL epitopes. (A) Spleen cells from TMEV-infected mice were stimulated in vitro for 5 days with the $VP2_{165–173}$ peptide and used as effector cells to assess lytic activity against L929-K^b or L929-D^b target cells loaded with the stimulating peptide. (B) CNS-IL were assayed ex vivo for the ability to lyse $VP3_{101–120}$-loaded L929-K^b and L929-D^b target cells. Spontaneous release was similar for both target cell lines used (≈10 to 15%).

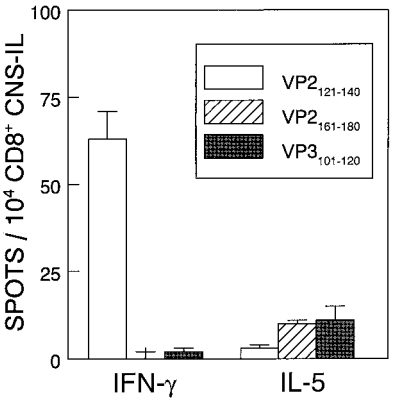

FIG. 6. Cytokine profiles of $CD8^+$ T cells specific for dominant and subdominant CTL epitopes. $CD8^+$ CNS-IL were magnetically separated and assayed by Elispot at 8 days postinfection for the production of either IFN-γ or IL-5 upon stimulation with each of the three CTL epitope peptides. Results are expressed as the mean number of spots above background (≤7 spots for both IFN-γ and IL-5) from triplicate wells. CNS preparations from naive mice contain few if any $CD8^+$ T cells, and no peptide-specific cytokine spots were detected above unstimulated control cultures. A representative experiment from four separate experiments is shown here. The presence and number of spots for each peptide correlated closely with the presence or absence of lytic activity, as responses to subdominant epitopes were not detectable in every experiment.

previously defined $VP2_{121–130}$ epitope bound the D^b molecule nearly as well as ($VP2_{111–130}$) or better than ($VP2_{121–140}$) the minimal 10-mer peptide (Fig. 1). Thus, regardless of the mechanism, the use of longer peptides proved effective in determining the predominant MHC class I binding regions within the capsid proteins of the BeAn strain of TMEV.

An earlier report (25) suggested that VP1 and VP2, but not VP3, were the primary targets of the CTL response to TMEV (DA strain) in C57BL/10 mice. Later work by this group and others (3, 9) defined $VP2_{121/122–130}$ as the predominant D^b-restricted epitope. We report here that in addition to the $VP2_{121–130}$ epitope, C57BL/6 mice also generate detectable CTL responses against two subdominant epitopes located on VP2 (amino acids 165 to 173) and VP3 (amino acids 110 to 120). We also observed that mice infected with either the DA strain of TMEV or encephalomyocarditis virus generate a CTL response to both the VP3 epitope defined here and the predominant $VP2_{121–130}$ epitope (data not shown). Thus, it appears that the CTL responses to these closely related cardioviruses are restricted to the same epitope regions.

No CTL activity was observed against any of the H-2^b class I binding VP1 peptides (Fig. 2), and Elispot analysis showed no cytokine production by CNS-IL against any of the VP1 peptides (data not shown). These data suggest that, in contrast to previous studies with the DA strain of TMEV, no $CD8^+$ T-cell epitopes exist within VP1 for BeAn-infected C57BL/6 mice. Thus, the CTL response generated against DA may differ from that against BeAn due to the sequence difference within the potential VP1 epitope or in the epitope-flanking regions that may affect antigen processing (54).

Another factor that may account for differences between the DA strain studies mentioned above and the work presented here involves the different methods used in these studies. For example, processing of viral antigen by transfected cell lines may not mimic in vivo processing by CNS cells. Thus, the absence of a lytic response against VP3 transfectants in the previous study (25) may reflect the inefficient presentation of VP3 epitopes in these cell lines rather than the lack of VP3-specific CTL in virus-infected mice. By using peptide-loaded target cells in our experiments, we have obviated the need for antigen processing by these target cells.

It is interesting that while both $VP3_{101–120}$ and $VP3_{110–120}$ sensitized target cells for lysis by CNS-IL, a peptide of intermediate length ($VP3_{104–120}$) did not (Fig. 4B). Also, CTL activity was higher against the $VP3_{101–120}$ peptide compared to $VP3_{110–120}$. While it is possible that the CNS-infiltrating T cells preferentially recognize the longer version of this peptide associated with D^b, this difference in activity may simply be due to differential processing of the two peptides into a smaller minimal epitope by target cells. Alternatively, differential solubility of the peptides, $VP3_{110–120}$ in particular, may partially contribute to these inconsistent observations. However, the lack of detectable CTL activity against $VP3_{111–130}$ (Fig. 2), $VP3_{111–120}$, and $VP3_{112–120}$, combined with the observed lytic

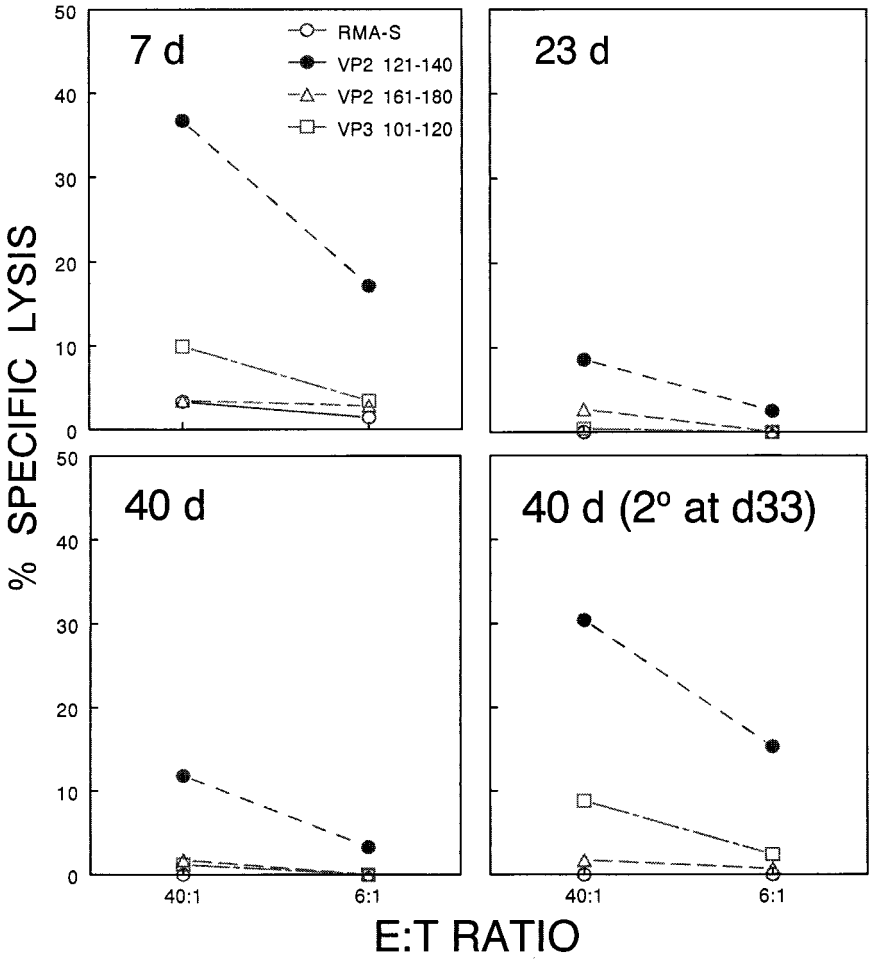

FIG. 7. Analysis of CTL response throughout the course of TMEV infection and during recall response to secondary virus challenge. CNS-IL were taken from TMEV-infected mice at different time points postinfection and assayed for lytic activity against RMA-S target cells loaded with the indicated peptides. Recall responses were measured in mice that received a second TMEV injection 33 days after the primary challenge (2° at d33). CTL assays were all done on the same day to minimize experimental variation. Similar reductions in CNS-infiltrating virus-specific $CD8^+$ T-cell responses over time were observed in three separate experiments, and a representative result is shown here. Spontaneous release was less than 13%.

activity against $VP3_{110–120}$, suggests that the minimal epitope must include residue 110.

The H-$2D^b$ molecule restricts CTL responses to the predominant epitope and the subdominant epitopes defined here (Fig. 5). Although antibodies to the D^b and K^b molecules are different and may not give the same level of sensitivity with respect to surface class I stabilization by peptide, it appears that both $VP2_{161–180}$ and $VP3_{101–120}$ can bind K^b as well as or better than D^b. Also, the minimal $VP2_{165–173}$ epitope was predicted based on the K^b binding motif. Nevertheless, CNS-IL were unable to lyse target cells bearing these peptides in conjunction with K^b. While preferential restriction of TMEV-specific CTL responses by D^b has been observed by others (24), the reason for this preference remains unclear. One possible explanation, as previously suggested (34), involves the differential expression of these two MHC molecules by antigen-presenting cells in either the CNS or the lymphoid tissues involved in initiating the anti-TMEV CTL responses. Lower K^b expression and higher D^b expression on such cells could selectively enhance the D^b-restricted response. Another possibility is that D^b-restricted CTL traffic more efficiently to the CNS than CTL specific for K^b-restricted epitopes. Both possibilities are consistent with the observation that K^b-restricted CTL are found in peripheral lymphoid organs but not in the CNS (24, 43).

Finally, the D^b-restricted CTL response may dominate or outcompete the K^b-restricted response just as $VP2_{121–130}$-specific CTL dominate the responses to the two epitopes defined here. However, *H-2D*$^{b-/-}$ mice are unable to mount a vigorous compensatory K^b-restricted response to TMEV (2), and these mice are susceptible to persistent infection. This suggests that the lack of K^b-restricted CTL in the CNS of normal C57BL/6 mice is not due simply to "competition" from D^b, but rather results from an intrinsic defect in the K^b-restricted virus-specific response.

Analysis of the capsid protein-specific $CD8^+$ T-cell response to the BeAn strain of TMEV in this study has led to the identification of two previously undefined epitopes and sug-

gests that a clear immunodominance hierarchy exists for the three defined epitopes: $VP2_{121–130}$ > $VP3_{101/110–120}$ > $VP2_{165–173}$. We report here that CTL specific for the two subdominant epitopes are present in the CNS by 7 to 8 days postinfection. Thus, the kinetics of this response parallels the rapid response to the immunodominant epitope. In addition, the recall response to $VP3_{101–120}$ and $VP2_{121–130}$ is identical to the primary response (Fig. 7), suggesting that the relative contribution of the subdominant CTL to the overall response does not change significantly upon secondary virus challenge.

Although the role of CTL specific for the subdominant epitopes defined here remains to be elucidated, studies of other virus-specific immune responses suggest that responses to subdominant CTL determinants can mediate at least partial protection against virus challenge (reviewed in reference 14). This may be especially important for the elimination of viral escape mutants that have undergone mutation within immunodominant epitopes or during chronic infections where the initial immunodominant CTL response proves insufficient for viral clearance. Thus, responses to nondominant viral epitopes may play a key role in clearing rapidly mutating RNA viruses such as TMEV (12), whose pathogenesis is associated with chronic viral infection.

In addition to direct lysis of infected cells, $CD8^+$ T cells also secrete cytokines such as IFN-γ and tumor necrosis factor alpha that may aid in the elimination of infectious virus from the host (17). We show here that CTL specific for $VP2_{121–130}$ produce IFN-γ, while CTL specific for the two subdominant epitopes produce mainly IL-5 (Fig. 6). The significance of this phenomenon with respect to resistance to TMEV-induced demyelinating disease and whether or not the Tc2-type cells specific for the epitopes defined here play any protective role in C57BL/6 mice are unclear. However, as Th1 cells appear to play a role in TMEV-induced demyelinating disease pathogenesis, it is easy to speculate that these Tc2-type cells may help to regulate the proinflammatory response directed against either viral or self-epitopes during the course of TMEV infection. Now that the specificity and function of these $CD8^+$ T cells are known, their precise role in the immune response to TMEV can be readily investigated.

ACKNOWLEDGMENTS

M. Lyman and H. Lee contributed equally to this work.

This work was supported by USPHS grants NS23349, NS28752, and NS33008.

REFERENCES

1. **Allen, I., and B. Brankin.** 1993. Pathogenesis of multiple sclerosis—the immune diathesis and the role of viruses. J. Neuropathol. Exp. Neurol. **52:**95–105.
2. **Azoulay-Cayla, A., S. Dethlefs, B. Perarnau, E. L. Larsson-Sciard, F. A. Lemonnier, M. Brahic, and J. F. Bureau.** 2000. *H-2D$^{b-/-}$* mice are susceptible to persistent infection by Theiler's virus. J. Virol. **74:**5470–5476.
3. **Borson, N. D., C. Paul, X. Lin, W. K. Nevala, M. A. Strausbauch, M. Rodriguez, and P. J. Wettstein.** 1997. Brain-infiltrating cytolytic T lymphocytes specific for Theiler's virus recognize $H2D^b$ molecules complexed with a viral VP2 peptide lacking a consensus anchor residue. J. Virol. **71:**5244–5250.
4. **Bureau, J. F., X. Montagutelli, F. Bihl, S. Lefebvre, J. L. Guenet, and M. Brahic.** 1993. Mapping loci influencing the persistence of Theiler's virus in the murine central nervous system. Nat. Genet. **5:**87–91.
5. **Clatch, R. J., R. W. Melvold, S. D. Miller, and H. L. Lipton.** 1985. Theiler's murine encephalomyelitis virus (TMEV)-induced demyelinating disease in mice is influenced by the H-2D region: correlation with TMEV-specific delayed-type hypersensitivity. J. Immunol. **135:**1408–1414.
6. **Cole, G. A., V. K. Clements, E. P. Garcia, and S. Ostrand-Rosenberg.** 1987. Allogeneic H-2 antigen expression is insufficient for tumor rejection. Proc. Natl. Acad. Sci. USA **84:**8613–8617.
7. **Dal Canto, M. C., R. W. Melvold, B. S. Kim, and S. D. Miller.** 1995. Two models of multiple sclerosis: experimental allergic encephalomyelitis (EAE) and Theiler's murine encephalomyelitis virus (TMEV) infection. A pathological and immunological comparison. Microsc. Res. Technol. **32:**215–229.
8. **Del Val, M., H. Volkmer, J. B. Rothbard, S. Jonjic, M. Messerle, J. Schickedanz, M. J. Reddehase, and U. H. Koszinowski.** 1988. Molecular basis for cytolytic T-lymphocyte recognition of the murine cytomegalovirus immediate-early protein pp89. J. Virol. **62:**3965–3972.
9. **Dethlefs, S., N. Escriou, M. Brahic, S. van der Werf, and E. L. Larsson-Sciard.** 1997. Theiler's virus and Mengo virus induce cross-reactive cytotoxic T lymphocytes restricted to the same immunodominant VP2 epitope in C57BL/6 mice. J. Virol. **71:**5361–5365.
10. **Dhib-Jalbut, S., and D. E. McFarlin.** 1990. Immunology of multiple sclerosis. Ann. Allergy **64:**433–444.
11. **Dillner, J.** 1994. Enzyme immunoassay detection of induction of MHC class I expression by synthetic peptides from the E6 and E7 regions of human papillomavirus type 16. J. Immunol. Methods **167:**195–205.
12. **Drake, J. W.** 1993. Rates of spontaneous mutation among RNA viruses. Proc. Natl. Acad. Sci. USA **90:**4171–4175.
13. **Eberl, G., J. Renggli, Y. Men, M. A. Roggero, J. A. Lopez, and G. Corradin.** 1999. Extracellular processing and presentation of a 69-mer synthetic polypeptide to MHC class I-restricted T cells. Mol. Immunol. **36:**103–112.
14. **Gallimore, A., H. Hengartner, and R. Zinkernagel.** 1998. Hierarchies of antigen-specific cytotoxic T-cell responses. Immunol. Rev. **164:**29–36.
15. **Gerety, S. J., W. J. Karpus, A. R. Cubbon, R. G. Goswami, M. K. Rundell, J. D. Peterson, and S. D. Miller.** 1994. Class II-restricted T cell responses in Theiler's murine encephalomyelitis virus-induced demyelinating disease. V. Mapping of a dominant immunopathologic VP2 T cell epitope in susceptible SJL/J mice. J. Immunol. **152:**908–918.
16. **Gerety, S. J., M. K. Rundell, M. C. Dal Canto, and S. D. Miller.** 1994. Class II-restricted T cell responses in Theiler's murine encephalomyelitis virus-induced demyelinating disease. VI. Potentiation of demyelination with and characterization of an immunopathologic $CD4^+$ T cell line specific for an immunodominant VP2 epitope. J. Immunol. **152:**919–929.
17. **Guidotti, L. G., T. Ishikawa, M. V. Hobbs, B. Matzke, R. Schreiber, and F. V. Chisari.** 1996. Intracellular inactivation of the hepatitis B virus by cytotoxic T lymphocytes. Immunity **4:**25–36.
18. **Inoue, A., Y. K. Choe, and B. S. Kim.** 1994. Analysis of antibody responses to predominant linear epitopes of Theiler's murine encephalomyelitis virus. J. Virol. **68:**3324–3333.
19. **Johnson, A. J., M. K. Njenga, M. J. Hansen, S. T. Kuhns, L. Chen, M. Rodriguez, and L. R. Pease.** 1999. Prevalent class I-restricted T-cell response to the Theiler's virus epitope D^b:$VP2_{121–130}$ in the absence of endogenous CD4 help, tumor necrosis factor alpha, gamma interferon, perforin, or costimulation through CD28. J. Virol. **73:**3702–3708.
20. **Kim, B. S., Y. K. Choe, M. A. Crane, and C. R. Jue.** 1992. Identification and localization of a limited number of predominant conformation-independent antibody epitopes of Theiler's murine encephalomyelitis virus. Immunol. Lett. **31:**199–205.
21. **Kim, B. S., J. P. Palma, A. Inoue, and C. S. Koh.** 2000. Pathogenic immunity in Theiler's virus-induced demyelinating disease: a viral model for multiple sclerosis. Arch. Immunol. Ther. Exp. **48:**373–379.
22. **Kim, B. S., R. L. Yauch, Y. Y. Bahk, J. A. Kang, M. C. Dal Canto, and C. K. Hall.** 1998. A spontaneous low-pathogenic variant of Theiler's virus contains an amino acid substitution within the predominant $VP1_{233–250}$ T-cell epitope. J. Virol. **72:**1020–1027.
23. **Kozlowski, S., M. Corr, M. Shirai, L. F. Boyd, C. D. Pendleton, J. A. Berzofsky, and D. H. Margulies.** 1993. Multiple pathways are involved in the extracellular processing of MHC class I-restricted peptides. J. Immunol. **151:**4033–4044.
24. **Lin, X., L. R. Pease, and M. Rodriguez.** 1997. Differential generation of class I H-2D- versus H-2K-restricted cytotoxicity against a demyelinating virus following central nervous system infection. Eur. J. Immunol. **27:**963–970.
25. **Lin, X., N. R. Thiemann, L. R. Pease, and M. Rodriguez.** 1995. VP1 and VP2 capsid proteins of Theiler's virus are targets of H-2D-restricted cytotoxic lymphocytes in the central nervous system of B10 mice. Virology **214:**91–99.
26. **Lindsley, M. D., R. Thiemann, and M. Rodriguez.** 1991. Cytotoxic T cells isolated from the central nervous systems of mice infected with Theiler's virus. J. Virol. **65:**6612–6620.
27. **Lipton, H. L., and M. C. Dal Canto.** 1976. Chronic neurologic disease in Theiler's virus infection of SJL/J mice. J. Neurol. Sci. **30:**201–207.
28. **Lipton, H. L., J. Kratochvil, P. Sethi, and M. C. Dal Canto.** 1984. Theiler's virus antigen detected in mouse spinal cord 2 1/2 years after infection. Neurology **34:**1117–1119.
29. **Ljunggren, H. G., N. J. Stam, C. Ohlen, J. J. Neefjes, P. Hoglund, M. T. Heemels, J. Bastin, T. N. Schumacher, A. Townsend, K. Karre, et al.** 1990. Empty MHC class I molecules come out in the cold. Nature **346:**476–480.

30. **Martinez-Kinader, B., G. B. Lipford, H. Wagner, and K. Heeg.** 1995. Sensitization of MHC class I-restricted T cells to exogenous proteins: evidence for an alternative class I-restricted antigen presentation pathway. Immunology **86:**287–295.
31. **Miller, S. D., C. L. Vanderlugt, W. S. Begolka, W. Pao, R. L. Yauch, K. L. Neville, Y. Katz-Levy, A. Carrizosa, and B. S. Kim.** 1997. Persistent infection with Theiler's virus leads to CNS autoimmunity via epitope spreading. Nat. Med. **3:**1133–1136.
32. **Murray, P. D., D. B. McGavern, X. Lin, M. K. Njenga, J. Leibowitz, L. R. Pease, and M. Rodriguez.** 1998. Perforin-dependent neurologic injury in a viral model of multiple sclerosis. J. Neurosci. **18:**7306–7314.
33. **Nicholson, S. M., M. C. Dal Canto, S. D. Miller, and R. W. Melvold.** 1996. Adoptively transferred $CD8^+$ T lymphocytes provide protection against TMEV-induced demyelinating disease in BALB/c mice. J. Immunol. **156:** 1276–1283.
34. **Njenga, M. K., L. R. Pease, P. Wettstein, T. Mak, and M. Rodriguez.** 1997. Interferon alpha/beta mediates early virus-induced expression of H-2D and H-2K in the central nervous system. Lab. Investig. **77:**71–84.
35. **Ostrand-Rosenberg, S., C. Roby, V. K. Clements, and G. A. Cole.** 1991. Tumor-specific immunity can be enhanced by transfection of tumor cells with syngeneic MHC-class-II genes or allogeneic MHC-class-I genes. Int. J. Cancer Suppl. **6:**61–68.
36. **Palma, J. P., Lee, H.-G., Kang, B.-S., Dal Canto, M., Miller, S. D., and B. S. Kim.** 2001. Enhanced susceptibility to Theiler's virus-induced demyelinating disease in perforin-deficient mice. J. Neuroimmunol. **116:**125–135.
37. **Pena Rossi, C., A. McAllister, L. Fiette, and M. Brahic.** 1991. Theiler's virus infection induces a specific cytotoxic T lymphocyte response. Cell. Immunol. **138:**341–348.
38. **Pevear, D. C., M. Calenoff, E. Rozhon, and H. L. Lipton.** 1987. Analysis of the complete nucleotide sequence of the picornavirus Theiler's murine encephalomyelitis virus indicates that it is closely related to cardioviruses. J. Virol. **61:**1507–1516.
39. **Pullen, L. C., and B. S. Kim.** 1991. Identification of a suitable target cell line for Theiler's murine encephalomyelitis virus specific CTL. FASEB J. **5:**A1094.
40. **Pullen, L. C., S. D. Miller, M. C. Dal Canto, and B. S. Kim.** 1993. Class I-deficient resistant mice intracerebrally inoculated with Theiler's virus show an increased T cell response to viral antigens and susceptibility to demyelination. Eur. J. Immunol. **23:**2287–2293.
41. **Rammensee, H. G., T. Friede, and S. Stevanoviic.** 1995. MHC ligands and peptide motifs: first listing. Immunogenetics **41:**178–228.
42. **Reinholdsson-Ljunggren, G., L. Franksson, T. Dalianis, and H. G. Ljunggren.** 1993. Identification of $H\text{-}2K^b$-, D^b- and D^d-binding peptides derived from amino acid sequences of polyoma virus T antigens. Int. J. Cancer **54:**992–995.
43. **Rodriguez, M., A. J. Dunkel, R. L. Thiemann, J. Leibowitz, M. Zijlstra, and R. Jaenisch.** 1993. Abrogation of resistance to Theiler's virus-induced demyelination in $H\text{-}2^b$ mice deficient in beta 2-microglobulin. J. Immunol. **151:**266–276.
44. **Rodriguez, M., J. Leibowitz, and C. S. David.** 1986. Susceptibility to Theiler's virus-induced demyelination. Mapping of the gene within the H-2D region. J. Exp. Med. **163:**620–631.
45. **Rodriguez, M., J. Leibowitz, and P. Lampert.** 1983. Persistent infection of oligodendrocytes in Theiler's virus induced encephalomyelitis. Ann. Neurol. **13:**426–433.
46. **Soldan, S. S., R. Berti, N. Salem, P. Secchiero, L. Flamand, P. A. Calabresi, M. B. Brennan, H. W. Maloni, H. F. McFarland, H. C. Lin, M. Patnaik, and S. Jacobson.** 1997. Association of human herpes virus 6 (HHV-6) with multiple sclerosis: increased IgM response to HHV-6 early antigen and detection of serum HHV-6 DNA. Nat. Med. **3:**1394–1397.
47. **Targoni, O. S., and P. V. Lehmann.** 1998. Endogenous myelin basic protein inactivates the high avidity T cell repertoire. J. Exp. Med. **187:**2055–2063.
48. **Townsend, A., C. Ohlen, L. Foster, J. Bastin, H. G. Ljunggren, and K. Karre.** 1989. A mutant cell in which association of class I heavy and light chains is induced by viral peptides. Cold Spring Harbor Symp. Quant. Biol. **54:**299–308.
49. **Townsend, A. R., F. M. Gotch, and J. Davey.** 1985. Cytotoxic T cells recognize fragments of the influenza nucleoprotein. Cell **42:**457–467.
50. **Wang, J., S. Saffold, X. Cao, J. Krauss, and W. Chen.** 1998. Eliciting T cell immunity against poorly immunogenic tumors by immunization with dendritic cell-tumor fusion vaccines. J. Immunol **161:**5516–5524.
51. **Yauch, R. L., K. Kerekes, K. Saujani, and B. S. Kim.** 1995. Identification of a major T-cell epitope within VP3 amino acid residues 24 to 37 of Theiler's virus in demyelination-susceptible SJL/J mice. J. Virol. **69:**7315–7318.
52. **Yauch, R. L., and B. S. Kim.** 1994. A predominant viral epitope recognized by T cells from the periphery and demyelinating lesions of SJL/J mice infected with Theiler's virus is located within VP1(233–244). J. Immunol. **153:**4508–4519.
53. **Yauch, R. Y., J. P. Palma, H. Yahikozawa, C.-S. Koh, and B. S. Kim.** 1998. Role of individual T cell epitopes of Theiler's virus in the pathogenesis of demyelination correlates with the ability to induce a Th1 response. J. Virol. **72:**6169–6174.
54. **Yellen-Shaw, A. J., E. J. Wherry, G. C. Dubois, and L. C. Eisenlohr.** 1997. Point mutation flanking a CTL epitope ablates in vitro and in vivo recognition of a full-length viral protein. J. Immunol **158:**3227–3234.